Korean J. Chem. Eng., **25**(5), 1184-1189 (2008)

Epitaxial growth of GaN on (0001) Al_2O_3 via solution-cast seed layer formation process using $Ga(mDTC)_3$

Do Hoon Kim*, Umme Farva*, Woo Sik Jung*, Eui Jung Kim, and Chinho Park*,†**

*School of Display and Chemical Engineering, Yeungnam University, Gyeongsan 712-749, Korea
**Department of Chemical Engineering, University of Ulsan, Ulsan 680-749, Korea
(*Received 11 September 2007 • accepted 14 February 2008*)

Abstract−This paper reports an alternative method for the growth of GaN epitaxial layer on (0001) Al_2O_3 substrate by hot-wall vapor phase epitaxy technique. Tris (N,N-dimethyldithiocarbamato)-gallium (III), $Ga(mDTC)_3$ was introduced as a precursor material for the seed layer formation in the growth of GaN. Optimal growth conditions with seed layers formed by the $Ga(mDTC)_3$ concentration of 0.047 mol/L were identified: Growth temperature was found to be 850 °C, and optimal distance between the reactant outlet and substrate was determined to be 12.5 cm. Characterization results showed that this growth method produce high-crystallinity GaN epitaxial layers at a relatively lower growth temperature compared to the existing growth techniques and simplify the growth process.

Key words: Hot-wall Vapor Phase Epitaxy, Gallium Nitride, $Ga(mDTC)_3$ Precursor, Solution Casting, Seed Layer Formation

INTRODUCTION

Recent progress in the nitride semiconductor technology has resulted in remarkable advances in materials quality and device performance [1]. Group III nitrides such as gallium nitride (GaN), indium nitride (InN) and aluminum nitride (AlN) are very promising materials for optoelectronic emitters, detectors and high power/temperature electronic devices [2-4].

Traditionally, nitride semiconductors have been deposited by vapor phase epitaxy techniques such as hydride vapor phase epitaxy (HVPE) [5,6], organometallic vapor phase epitaxy (OMVPE) [7,8] and molecular beam epitaxy (MBE) [9]. There have been also several reports to prepare GaN crystal structures by using solution growth under the high nitrogen pressure (10-20 kbar) [10] or by sublimation [11]. In some cases GaN epitaxy at decreased temperatures was also achieved by using methylized hydrazine derivatives such as $(CH_3)_2NNH_2$ [12] and $(CH_3)(H)NNH_2$ [13].

Owing to the lack of a natural substrate, most of the GaN devices are made from multiple hetero-epitaxial layers grown on commercially available substrates. The most widely used substrates for the III-nitride epitaxy are sapphire [14-16] and silicon carbide [17]. It was observed that a poor lattice match and large difference in thermal expansion coefficients for these substrates usually leads to high dislocation densities, formation of threading defects, and residual strains, all of which affect both optical and electrical properties of the devices [18]. The ongoing effort to improve the GaN film properties, therefore, has driven the research community to explore alternative substrate materials and growth techniques.

HVPE is preferred for growing thick GaN layers and free-standing bulk GaNs, which may serve as quasi-substrates for the growth of device structures by minimizing the in-plane anisotropy of the lattice constants. Besides, it has been recently demonstrated that HVPE can also be used to grow high-quality thin GaN layers on sapphire ($d \leq 10$ μm with a dislocation density of $\sim 1 \times 10^8$ cm^{-2}) using a two-step procedure similar to that of OMVPE [19]. Modified hydride vapor phase epitaxy (MHVPE) is a technique of using TMGa, HCl, and NH_3 as the precursors for the epitaxial growth of thin or thick GaN films in a hot-wall reactor configuration used in HVPE by utilizing the benefits of two conventional growth techniques, i.e., OMVPE and HVPE. This method demonstrated a successful growth of high-crystallinity GaN along with good process controllability and high growth rate [20].

Vapor phase epitaxy techniques utilize either seed or buffer layer between the substrate and GaN film to minimize the mismatch in lattice constants and thermal expansion coefficients. Including these interface layer, however, complicates the growth process due to additional process steps involved. The reactor heat-up and cool-down cycle has to be incorporated to accommodate the seed or buffer layer deposition, which complicates the overall growth process and lowers the production yield and throughput. Therefore there is a need for the development of an alternative process to simplify the growth runs, which would eventually reduce the production cost.

In this manuscript we report the growth of GaN epitaxial layers by MHVPE technique using a seed layer formed by spin-coating of a precursor solution, tris (N,N-dimethyldithiocarbamato)-gallium (III), $Ga(mDTC)_3$ in chloroform on the Al_2O_3 substrate. The optimized growth conditions are first explored and further confirmed by SEM, XRD and PL measurements.

EXPERIMENTAL

The $Ga(mDTC)_3$ precursor was synthesized by dissolving Ga $(NO_3)_3 \cdot xH_2O$ (x~7.6) and sodium N,N-dimethyldithiocarbamate dihydrate (TCI) (1 : 3 mole ratio of the Ga salt to the ligand) in methanol and recrystallized in chloroform [21].

The GaN epi-layers were grown by the MHVPE technique, and the detailed description of the process and schematic illustration of the MHVPE system is shown in the previous work [22]. In the MHVPE system, the reactor has hot-wall design, housed in a clamshell fur-

†To whom correspondence should be addressed.
E-mail: chpark@ynu.ac.kr

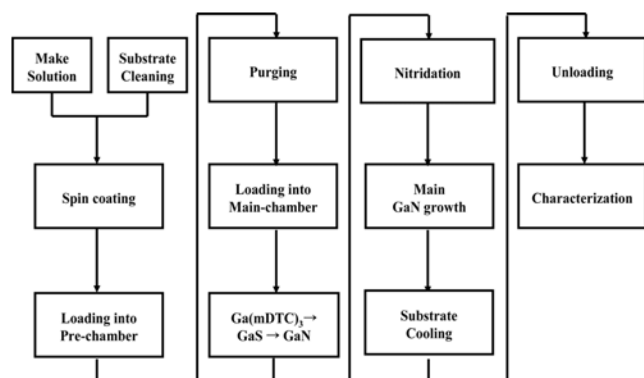

Fig. 1. Growth sequence of GaN thin films using $Ga(mDTC)_3$ solution-cast process.

nace with six independently controlled temperature zones. Each of the gas inlet tubes is made of quartz, and all are concentric, with the center tubes having adjustable lengths so that the reaction temperatures can be controlled by adjusting either the inserted tube lengths or the furnace zone temperatures. The typical growth sequence used in the experiments of this study is shown in the Fig. 1.

Commercially available (0001) Al_2O_3 substrate, cut in $10\times10\ mm^2$ size, was degreased, cleaned and rinsed in hot TCE, acetone and methyl alcohol for 5 min, respectively, ultrasonicated in methanol for 5 min, and dried by N_2 blow-drying. The prepared $Ga(mDTC)_3$ precursor solution at a specific concentration was spin-coated on the cleaned and dried substrate. The substrate was then loaded into the pre-chamber, and it was subsequently transferred to the main growth chamber through load-lock bar. The substrate was first heated to the nitridation temperature under ambient nitrogen, followed by the nitridation step for 10 min in ambient NH_3/N_2. After the nitridation step, TMGa and HCl were added simultaneously to the reactant stream to initiate the growth of GaN epitaxial layers. The total gas flow rate was maintained at 2915 sccm, and the reactor was kept at 1 atmospheric pressure. After the growth, the substrate was cooled in NH_3/N_2 environment to minimize the defect generation by partial decomposition of the GaN film surface.

Parametric growth studies were performed to determine the optimum conditions of growth temperature, the distance between the reactant outlet and substrate (z-position), $Ga(mDTC)_3$ precursor solution concentration and its spin-coating speed, the HCl/TMGa ratio, and TMGa-bath temperature. Details of the experimental conditions are described in Table 1. The morphologies of the grown GaN films were observed by scanning electron microscopy (SEM). The crystallinity and optical quality of the grown films were analyzed by X-ray diffraction (XRD) and photoluminescence (PL) measurements.

RESULTS AND DISCUSSION

The growth parameters were systematically optimized by changing various process conditions including the spin-coating rpm, growth temperature, z-position, $Ga(mDTC)_3$ precursor concentration, etc. as described in the previous section. First, the spin-coating speed of precursor solution was investigated, and it was found that the best surface morphology was obtained at ~2000 rpm for the range of precursor solution concentration investigated. The spin-coating time was fixed at 30 sec based on the results of preliminary growth runs. The range of parameters varied in this study together with other fixed process conditions are summarized in Table 1.

The spin-coated $Ga(mDTC)_3$/chroroform solution forms the solution-cast seed layer upon evaporation of solvent during the reactor heat-up sequence followed by the nitridation step. The precursor, $Ga(mDTC)_3$ first decomposes into Ga_2S_3 which has a defected zinc-blende structure, and it further converts into GaN under NH_3 environment as the temperature increases (as shown in Eq. (1)) [21].

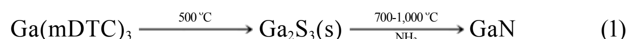

$$Ga(mDTC)_3 \xrightarrow{500\,^{\circ}C} Ga_2S_3(s) \xrightarrow[NH_3]{700\text{-}1{,}000\,^{\circ}C} GaN \quad (1)$$

The deposition of GaN thin film on (0001) Al_2O_3 substrate by MHVPE technique is proceeded by the overall reactions shown in Eq. (2).

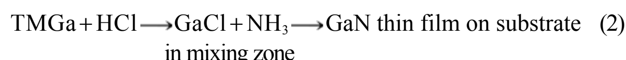

$$TMGa + HCl \longrightarrow \underset{\text{in mixing zone}}{GaCl} + NH_3 \longrightarrow \text{GaN thin film on substrate} \quad (2)$$

The axial centerline temperature profiles of the reactor used in

Table 1. Fixed and varied process conditions of this work for the growth of GaN epi-layers

Fixed \ Varied	Growth temperature	Z-position	$Ga(mDTC)_3$ conc.	Inlet HCl/TMGa ratio	TMGa-bath temp.
TMGa partial pressure	7.21×10^{-4} atm	7.21×10^{-4} atm	7.21×10^{-4} atm	7.21×10^{-4} atm	3.02×10^{-4}-7.21×10^{-4} atm
NH_3 partial pressure	5.83×10^{-2} atm	5.83×10^{-2} atm	5.83×10^{-2} atm	5.83×10^{-2} atm	2.44×10^{-4}-5.83×10^{-2} atm
HCl partial pressure	8.92×10^{-4} atm	8.92×10^{-4} atm	8.92×10^{-4} atm	1.20×10^{-3}-5.83×10^{-2} atm	4.12×10^{-4}-9.95×10^{-4} atm
TMGa-bath temp.	5 °C	5 °C	5 °C	5 °C	−10-5 °C
Inlet NH_3/TMGa ratio	81	81	81	81	81
Inlet HCl/TMGa ratio	1.24	1.24	1.24	1.24-1.66	1.38
Growth time	30 min	30 min	30 min	30 min	60 min
Growth temperature	700-970 °C	850 °C	850 °C	850 °C	850 °C
Z-position	15 cm	10-20 cm	12.5 cm	12.5 cm	12.5 cm
$Ga(mDTC)_3$ conc.	0.093 mol/L	0.093 mol/L	0.035-0.093 mol/L	0.070 mol/L	0.070 mol/L

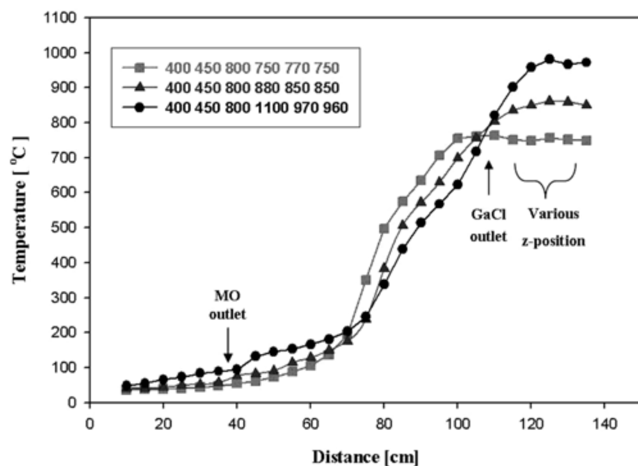

Fig. 2. Axial centerline temperature profiles of MHVPE reactor for the growth of GaN: 750 °C, 850 °C, and 970 °C.

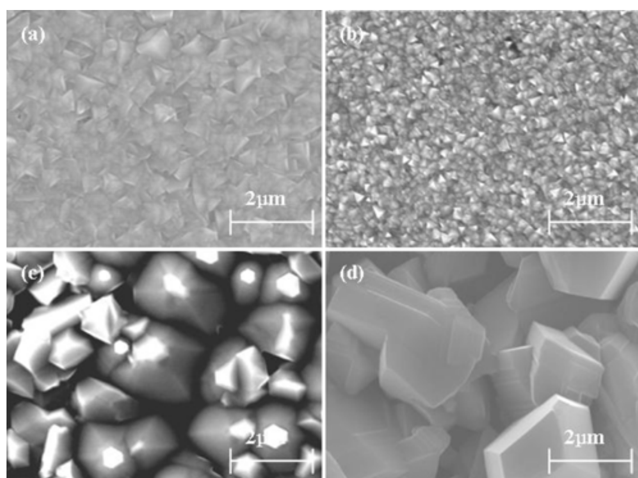

Fig. 3. SEM images of GaN epi-layer surfaces grown at various temperatures: (a) 700 °C, (b) 750 °C, (c) 850 °C, and (d) 970 °C.

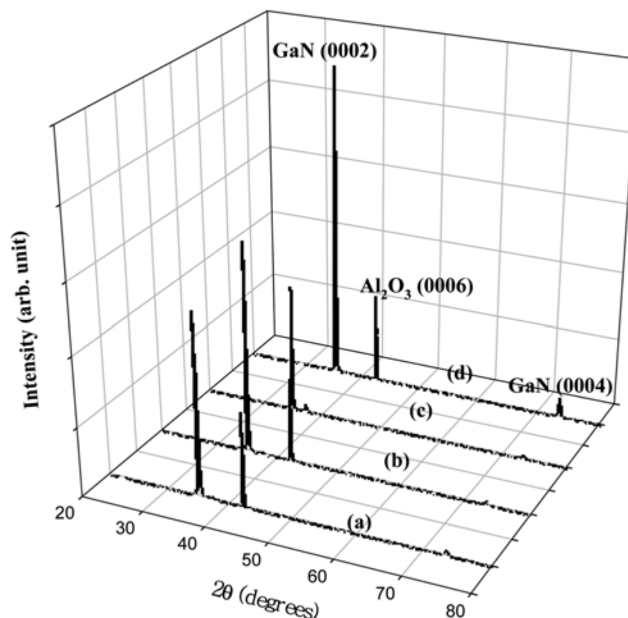

Fig. 4. X-ray diffraction patterns of GaN epi-layers grown at various temperatures: (a) 700 °C, (b) 750 °C, (c) 850 °C, and (d) 970 °C.

this study are described in Fig. 2 for the three cases of substrate temperatures (750 °C, 850 °C, and 970 °C). It is shown from the figure that the temperature flat zones (set point temperature ±5 °C) exceed 10 cm for the substrate temperatures investigated in this study, and also the thermal history of incoming reactant streams (i.e., temperature profile in the gas flow direction) is not significantly affected by the substrate temperature set point change, thus allowing experiments at different growth temperatures without altering the seed layer formation process.

Fig. 3 shows the SEM images of GaN thin film surfaces grown at various temperatures of 700 °C, 750 °C, 850 °C and 970 °C, respectively. The $Ga(mDTC)_3$ solution concentration was fixed at 0.093 mol/L for these runs. The SEM images show that the film morphology drastically changes as the growth temperature increases. It is also seen in the figure that the substrates are covered by dense GaN epi-layers for all the temperatures investigated. Large crystal grains with hexagonal phase begin to appear at and above 850 °C (Fig. 3(c) and 3(d)). At the early stage of epi-layer growth on seeded substrate, lattice strain and surface free energy play a crucial role in determining whether the growth proceeds via layer-by-layer growth mode (Frank-Van der Merwe), islanding mode (Volmer-Weber) or layer-by-layer growth followed by islanding mode (Stranski-Krastanov) [23]. The initial stage of growth involving nucleus generation is governed by the lattice strain and surface free energy, which eventually determines the film morphology. The seed layer formed by the solution-cast process of this study is thus closely related to the initial stage of growth in the aspect of controlling lattice strain and surface energy. It was inferred from the results that the films grown at 700 °C and 750 °C originated from Frank-Van der Merwe growth mode, while the films grown at 850 °C and above followed Volmer-Weber or Stranski-Krastanov mode. Fig. 4 shows the XRD patterns of the grown GaN epi-layers at 700 °C, 750 °C, 850 °C and 970 °C, respectively. Two distinct diffraction peaks were observed in all the samples indexed at (0002) and (0004), showing typical single-crystal Wurtzite GaN phases. The films grown at 700 °C, 750 °C and 970 °C showed an additional peak of (0006) Al_2O_3 with varying intensity, which indicates that the grown GaN epi-layers are relatively thin for 700 °C and 750 °C runs and the epi-layer does not cover the substrate surface entirely for 970 °C runs. The films grown at 850 °C, however, did not show the additional peak, indicating that the substrate surface was completely covered by predominantly crystalline hexagonal Wurtzite GaN. The difference in film morphology with respect to growth temperature is believed to be caused by the combined effect of seed floors formed by the solution-cast process of this study and the initial stage of growth provided at different temperatures.

Fig. 5 shows the SEM images of GaN thin films grown at 850 °C with the variation of the z-position. It was found that the film morphology strongly depends on the z-position, and the optimum distance between the reactant (GaCl) outlet and substrate is near 12.5

cm at 850 °C growth temperature. The z-position should be properly set to produce mirror surface of GaN with high crystallinity, since the concentration of gas phase film precursors (i.e. GaCl and NH_3) and their super-saturation degree varies along with the flow direction due to the radial and axial dispersions of the precursors. It is well known that the gas dynamics and mass transfer of reacting species play important role in determining the surface morphology of the grown film [19]. From the SEM image it is speculated that the GaN growth in this set of experiments is yet from optimum in terms of surface roughness and thus requires further optimization. Relevant XRD studies indicated that films grown at 850 °C with different z-positions are all single crystalline in nature except the films grown at the z-position of 20 cm. The room temperature PL spectra were measured for GaN films by the He-Cd laser with the excitation wavelength of 325 nm. Fig. 6 depicts the room temperature PL spectra of GaN films grown at 850 °C with z-position varying from 10 cm to 20 cm. The $Ga(mDTC)_3$ concentration was again maintained at 0.093 mol/L. It was shown that the strong near-band emission peak was observed near 3.4 eV for the samples grown in the z-position range 10 to 17.5 cm, while samples grown at 20 cm did not show any PL spectra. Yellow band spanning the range 2.11 to 2.43 eV was minimal or non-existent for the samples grown in the z-position range of 10 to 15 cm, while films grown at the z-position of 17.5 cm revealed noticeable yellow band. From the PL spectra, we could confirm that the most optimized and high crystalline growth was achieved when the sample was grown at the z-position of 12.5 cm.

Based on the parametric studies of growth temperature and z-position, it was concluded that GaN growth by MHVPE technique

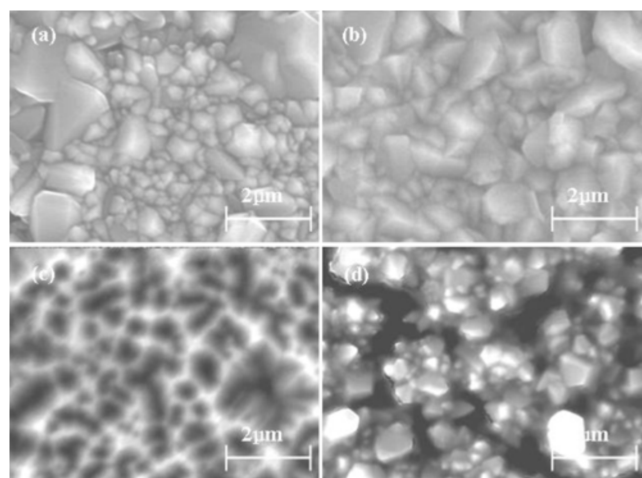

Fig. 5. SEM images of GaN epi-layers grown at optimized temperature of 850 °C with different z-positions: (a) 10 cm, (b) 12.5 cm, (c) 17.5 cm, and (d) 20 cm. The $Ga(mDTC)_3$ concentration is fixed at 0.093 mol/L.

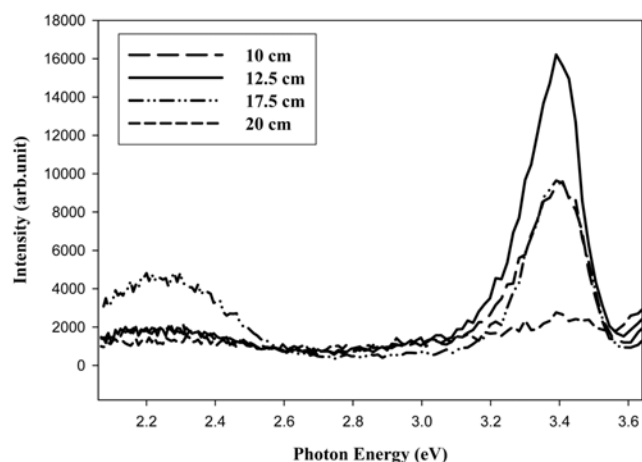

Fig. 6. Room temperature PL spectra of GaN epi-layers grown at optimized temperature of 850 °C with different z-positions: (a) 10 cm, (b) 12.5 cm, (c) 17.5 cm, and (d) 20 cm.

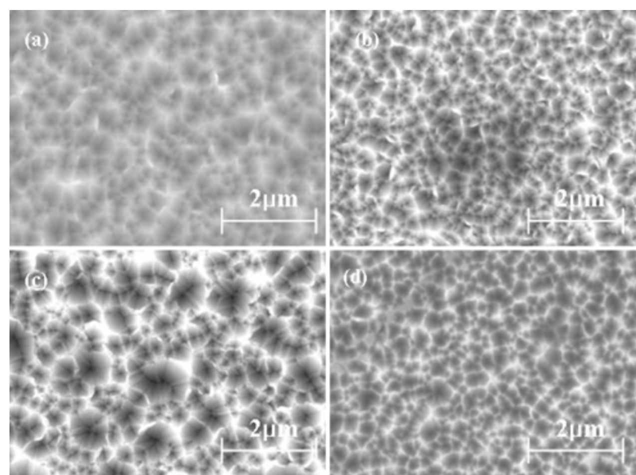

Fig. 7. SEM images of GaN epi-layers grown at various HCl/TMGa ratios: (a) 1.24, (b) 1.38, (c) 1.52, and (d) 1.66. The $Ga(mDTC)_3$ concentration is fixed at 0.070 mol/L.

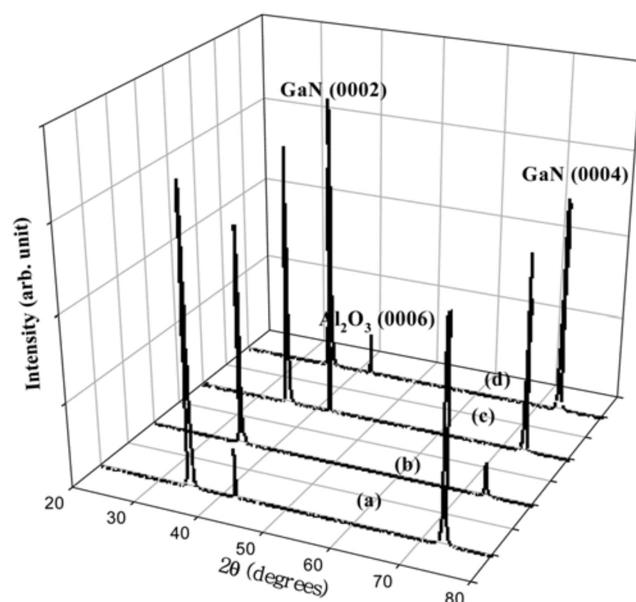

Fig. 8. X-ray diffraction patterns of GaN epi-layers grown at various HCl/TMGa ratios: (a) 1.24, (b) 1.38, (c) 1.52, and (d) 1.66. The $Ga(mDTC)_3$ concentration is fixed at 0.070 mol/L.

via solution-cast seed layer formation process provides a wide process window for single crystal thin film deposition with device-grade optical property, but it requires further improvement in surface roughness. Frank-Van der Merwe mode 2-dimensional growth is preferred for mirror surface production which is crucial to the opto-electronic device applications. To promote 2-D growth, seed layer formation process and gas phase super-saturation degree control were, therefore, further investigated. First, we repeated growth runs at optimized conditions with different $Ga(mDTC)_3$ concentrations varying from 0.035 to 0.093 mol/L and found that 0.070 mol/L produces the best samples in terms of crystallinity, optical quality and surface morphology.

SEM surface images of GaN films grown at four different HCl/TMGa ratios (1.24, 1.38, 1.52 and 1.66) are shown in Fig. 7. Increase of the HCl/TMGa ratio was expected to lower the gas phase super-saturation degree and thus prefer the 2-D growth mode. The surface morphologies shown in the figure clearly show that the substrates were covered by GaN thin film and 2-D growth was enhanced as expected. XRD patterns of these GaN thin films grown on (0001) Al_2O_3 substrate at different HCl/TMGa ratios (Fig. 8) also revealed that the epitaxial GaN films are highly oriented along the [0001] direction of the wurtzite GaN with excellent crystallinity. Finally the TMGa-bath temperature was varied in a decreasing fashion to

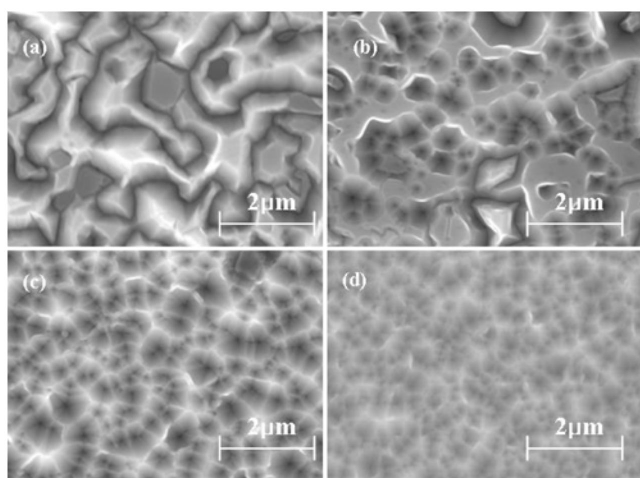

Fig. 9. SEM images of GaN epi-layers grown at various TMGa-bath temperatures: (a) −10 ºC, (b) −5 ºC, (c) 0 ºC, and (d) 5 ºC. The $Ga(mDTC)_3$ concentration is fixed at 0.070 mol/L.

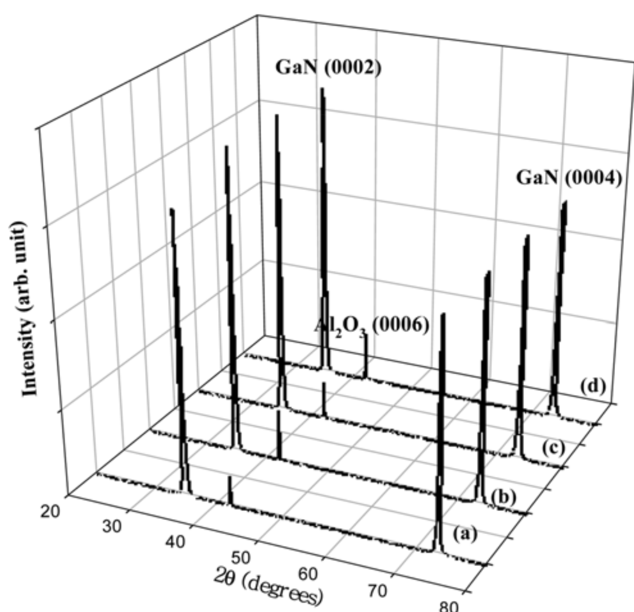

Fig. 10. X-ray diffraction patterns of GaN epi-layers grown at various TMGa-bath temperatures: (a) −10 ºC, (b) −5 ºC, (c) 0 ºC, and (d) 5 ºC. The $Ga(mDTC)_3$ concentration is fixed at 0.070 mol/L.

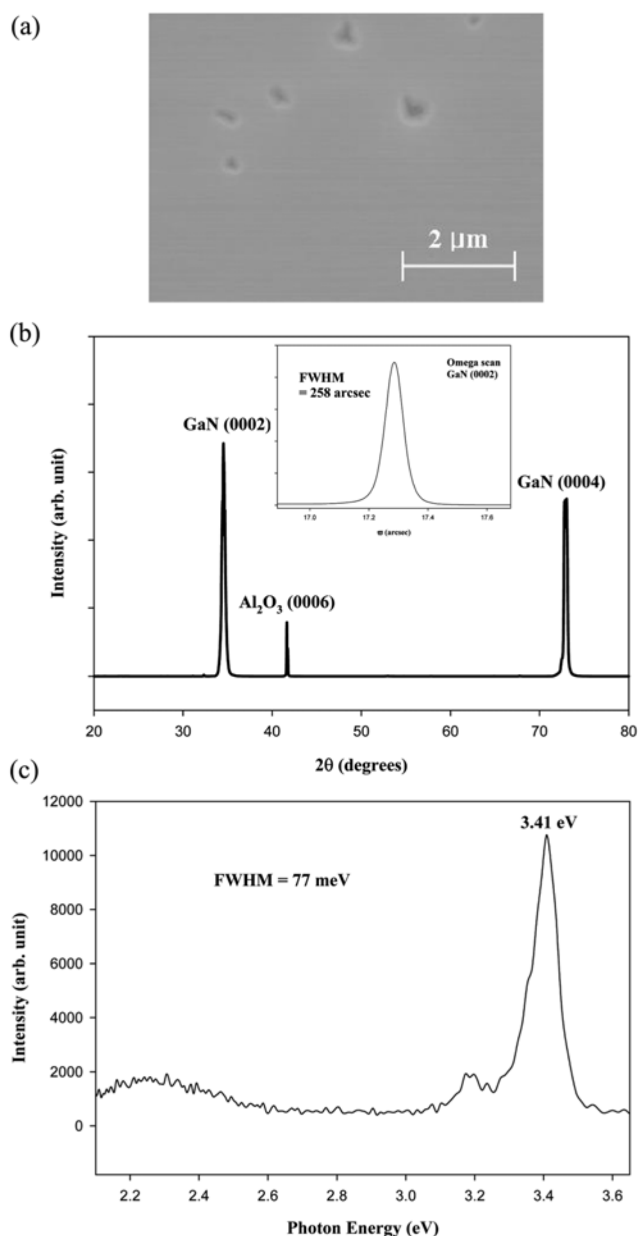

Fig. 11. Characterization results of GaN samples with optimized process conditions: a) SEM image, b) XRD pattern, c) PL spectrum. Corresponding values representing the quality of sample are included in the figures.

further decrease the gas phase super-saturation degree and to enhance the surface diffusivity of ad-species on the surface. The surface morphology and crystallinity of GaN thin films of this set of growth runs are shown in Fig. 9 and Fig. 10, respectively, and it was shown that 2-D growth is enhanced over the wide range of TMGa-bath temperature. After completing the systematic variation of process parameters, the optimum process conditions were finally identified as follows: The $Ga(mDTC)_3$ concentration of 0.047 mol/L, growth temperature of 850 °C, z-position of 12.5 cm, HCl/TMGa ratio of 1.38 with HCl/NH_3 ratio of 81, and TMGa-bath temperature of 5 °C. The surface morphology, crystallinity, optical quality of the optimized growth runs at the above-mentioned condition are shown in Fig. 11. As clearly shown in the figure, the method developed in this study proved to be a successful alternative way to produce mirror surface, device-quality epitaxial GaN thin films at relatively lower temperature.

One of other advantages of the solution-cast seed layer formation process which should be mentioned is the simplification of its growth process. The new method developed in this study eliminates the seed or buffer layer growth process steps typically involved in the vapor phase epitaxy techniques. The method reduces the overall growth time and simplifies the growth sequence. The method is also expected to provide better run to run reproducibility of the growth process, which will eventually reduce the production cost.

CONCLUSION

A solution-cast seed layer formation process was developed in this study and was applied for the growth of GaN thin films. It was proven to be a successful alternative method of providing GaN thin films having several merits in the GaN production sense. Composition control of $Ga(mDTC)_3$ precursor was crucial to visualize mirror surface GaN thin films with properly managed growth parameters. The method was applied for the GaN growth by MHVPE technique with $Ga(mDTC)_3$ seed layers, but other VPE techniques such as conventional HVPE and OMVPE can as well adopt this new seed layer formation process.

ACKNOWLEDGMENTS

This research was supported by the Yeungnam University research grants in 2007, and the researchers involved in this work were supported partially by the 2nd phase of the BK21 Program.

REFERENCES

1. S. Nakamura, M. Senoh, S.-i. Nagahama, N. Iwasa, T. Yamada, T. Matsushita, H. Kiyoku, Y. Sugimoto, T. Kozaki, H. Umemoto, M. Sano and K. Chocho, *Appl. Phys. Lett.*, **72**, 2014 (1998).
2. H. Morkoc, *Nitride semiconductors and devices*, Springer, Heidelberg (1999).
3. S. N. Mohammad and H. Morkoc, *Prog. Quantum Electron*, **20**, 361 (1996).
4. H. Morkoc, A. Di Carlo and R. Cingolani, in *Condensed matter news*, edited by Patrick Bernier (in press).
5. H. P. Maruska and J. J. Tietjen, *Appl. Phys. Lett.*, **15**, 327 (1969).
6. R. J. Molnar, W. Goetz, L. T. Romano and N. M. Johnson, *J. Cryst. Growth*, **178**, 147 (1997).
7. H. M. Manasevit, F. M. Erdmann and W. I. Simpson, *J. Electrochem. Soc.*, **118**, 1864 (1971).
8. M. Hashimoto, H. Amano, N. Sawaki and I. Akasaki, *J. Cryst. Growth*, **68**, 163 (1984).
9. S. Yoshida, S. Misawa and A. Itoh, *Appl. Phys. Lett.*, **26**, 461 (1975).
10. S. Porowsky and I. Grezegory, *J. Cryst. Growth*, **178**, 174 (1997).
11. S. Kurai, Y. Naoi, T. Abe, S. Ohmi and S. Sakai, *Jpn. J. Appl. Phys.*, **35**, L77 (1996).
12. H. Sato, H. Takahashi, A. Watanabe and H. Ota, *Appl. Phys. Lett.*, **68**, 3617 (1996).
13. H. Tsuchiya, A. Tageuchi, M. Kurihara and F. Hasegawa, *J. Cryst. Growth*, **152**, 21 (1995).
14. J. Lee, H. Paek, J. Yoo, G. Kim and D. Kum, *Mat. Sci. Eng.*, **B59**, 12 (1999).
15. P. R. Tavernier and D. R. Clarke, *J. Am. Ceram. Soc.*, **85**, 49 (2002).
16. Y. Oshima1, T. Eri, M. Shibata, H. Sunakawa and A. Usui, *Phys. Stat. Sol. (a)*, **194**, 554 (2002).
17. A. Able, W. Wegscheider, K. Engl and J. Zweck, *J. Cryst. Growth*, **276**, 415 (2005).
18. T. Paskova1, P. P. Paskov, V. Darakchieva, S. Tungasmita, J. Birch and B. Monemar, *Phys. Stat. Sol. (a)*, **183**, 197 (2001).
19. D. Martin, J. Napierala, M. Ilegems, R. Butté and N. Grandjean, *Appl. Phys. Lett.*, **88**, 241914 (2006).
20. O. Kryliouk, M. Reed, T. Dann, T. Anderson and B. Chai, *Mater. Sci. Eng.*, **B66**, 26 (1999).
21. W. S. Jung, C. S. Ra and B. K. Min, *Bull. Korean Chem. Soc.*, **26**, 131 (2005).
22. C. Park, S. Yeo, J. H. Kim, D. Yoon and T. J. Anderson, *Thin Solid Films*, **498**, 94 (2006).
23. M. Copel, M. C. Reuter, E. Kaxiras and R. M. Tromp, *Phys. Rev. Letters*, **63**, 632 (1989).